

# Sensitivity Study for Atmospheric Applications with APEX

Johannes W. Kaiser, Jens Nieke, Daniel Schläpfer, Jason Brazile,  
and Klaus I. Itten

University of Zurich, Remote Sensing Laboratories, Zurich, Switzerland

`jkaiser@geo.unizh.ch`, `nieke@geo.unizh.ch`, `dschlapf@geo.unizh.ch`,

`jbrazile@geo.unizh.ch`, and `itten@geo.unizh.ch`

## Abstract

The new airborne imaging spectrometer APEX will be available in 2006. It observes the visible and short-wave infrared spectral ranges. With its unique combination of spectral and spatial resolution, atmospheric molecular spectroscopy is feasible with unprecedented spatial resolution and coverage. Sensitivity calculations show, that abundances of CO<sub>2</sub> and CH<sub>4</sub> and pollution events of NO<sub>2</sub> and O<sub>3</sub> in the planetary boundary layer will be quantified with a spatial resolution of several meters. Such observations open new possibilities in the characterization of sub-satellite pixel distributions and air pollution monitoring.

## Introduction

### The APEX Instrument

The Airborne Prism EXperiment (APEX) is an airborne dispersive pushbroom imaging spectrometer for the hyperspectral observation of ground reflectances [e.g. Nieke et al., 2004]. APEX is currently being built in a joint Swiss/Belgian project funded through the ESA PRODEX program. It will be operated by VITO, Belgium, starting from 2006.

The spectrometer records up to 511 spectral points in the wavelength range 380–2500 nm with a sampling interval of 0.4 to 10 nm. A CCD and a CMOS are used as detectors in the visible and SWIR spectral range, respectively. The ground pixel size ranges from 2 to 5 m corresponding to flight altitudes of 4 to 10 km. Since APEX is a pushbroom instrument all spectral points are simultaneously observed for all 1000 across-track pixels. A dedicated calibration laboratory is being built to facilitate the absolute calibration of the instrument. For more details visit the instrument homepage <http://www.apex-esa.org>.

### Atmospheric Applications

Even though APEX primarily aims at the observation of the surface reflectance, atmospheric applications have already been taken into account during the definition of the instrument requirements [Schläpfer and Schaepman, 2002]. APEX achieves an unprecedented combination of good spatial and spectral resolutions, coverage, and signal to noise ratio. Thus a large number of atmospheric parameters may also be retrieved from its measurements. Figure 1 gives an overview of the optical depths of various atmospheric constituents in the spectral range of APEX. The values are convolved to the spectral resolution of APEX. Its center band wavelengths are indicated by vertical red lines.

### Clouds

APEX may be used to observe variations in the radiance field due to the scattering by structured clouds at spatial scales ranging from about 1 m to several km simultaneously. E.g., von Savigny et al.

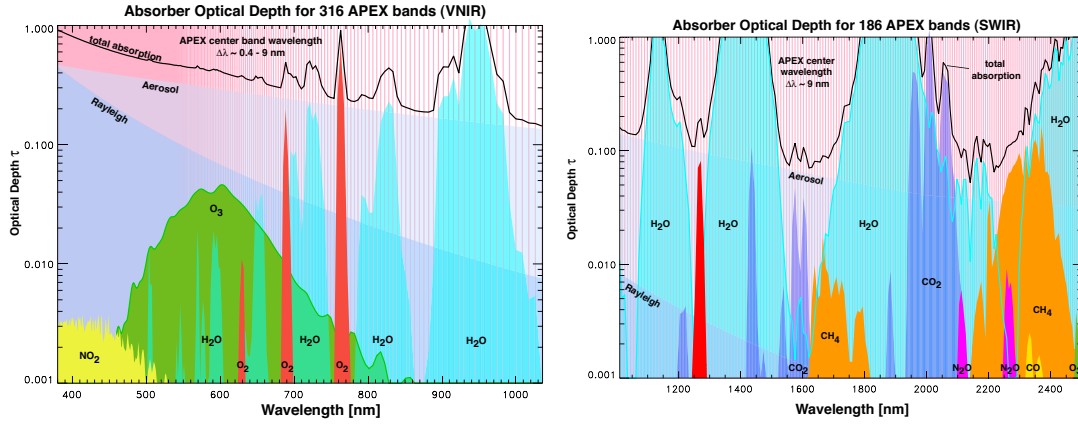


Figure 1: Atmospheric Constituents' Optical Depths Seen by APEX' VNIR and SWIR channels. (Reproduced from Kaiser et al. [2004])

[2002] have analyzed the radiative smoothing using a time series of zenith sky radiances under clouds. With APEX the analysis can be extended by observing a 2-dimensional field up-welling radiances over a large spectral range.

### Aerosols

The optical depth of typical aerosols displays a spectrally smooth signature. However, the optical depth varies considerably over the relatively large spectral range observed by APEX. Since a large number of aerosol retrieval algorithms established for existing satellite sensors can be applied to APEX observations, the aerosol product can be improved by combining information extracted with several algorithms, e.g. from Höller et al. [2004], von Hoyningen-Huene et al. [2003], Kaufman et al. [1997].

### Trace Gases

Owing to APEX' relatively good spectral resolution the spectral signatures of several trace gases can be observed. The optical depths of water vapor and carbon dioxide obviously display strong signatures that can be analyzed in the observed spectra. They can be used for the atmospheric correction of the observation during the retrieval of the surface reflectance.

Nitrogen dioxide, ozone, and methane have optical depths that are hardly discernible in the total optical depth. They are, however, of particular importance for the monitoring of local and regional air pollution [e.g. Schaub et al., 2005, Heldstab et al., 2004].

Tropospheric CO<sub>2</sub>, H<sub>2</sub>O have already been observed with the air-borne imaging spectrometer AVIRIS [Marion et al., 2004]. NO<sub>2</sub> has been measured with a ground-based imaging spectrometer in the plume of a power plant [Lohberger et al., 2004] and with a non-imaging air-borne spectrometer citepheue04a. However, none these measurements achieve the versatility, precision, and spatial resolution promised by APEX.

### This Paper

In this paper, we propose a method for observing H<sub>2</sub>O and tropospheric pollution by NO<sub>2</sub>, O<sub>3</sub>, CO<sub>2</sub>, and CH<sub>4</sub> with APEX. We calculate and present the theoretical precision and correlations of such measurements.

# Methods

## Proposed Retrieval Method

The well-established technique of Differential Optical Absorption Spectroscopy (DOAS) [Platt, 1994] retrieves the atmospheric trace gas contributions from the high-frequency component of the logarithm of the observed radiance in dedicated spectral fitting windows. It employs a so-called Air Mass Factor (AMF), which is assumed to be constant throughout the fit window. This assumption is generally bad in the near infrared spectral region [e.g. Buchwitz et al., 2000]. Furthermore, variations of the molecular absorption cross section with altitude cannot properly be accounted for [e.g. Sioris et al., 2004].

We propose to maintain the advantages of DOAS and overcome its limitations by fitting the atmospheric parameters directly to the high-frequency component of the logarithm of the observed radiance in dedicated fitting windows:

1. Take the logarithm  $\ln(I)$  observed radiance  $I$ . The relative depth of the molecular absorption features in the reflected radiance is independent of the (unknown) surface reflectance, i.e. characteristic of the atmosphere alone. This step transforms the absorption feature such that it has an absolute depth that is independent of the surface.
2. Fit a polynomial  $P_d(\lambda)$  of low degree  $d$  in the wavelength  $\lambda$  dimension to  $\ln(I(\lambda))$ .
3. Subtract the polynomial:  $\ln(I(\lambda)) - P_d(\lambda)$ . This removes most of the broadband influences of atmospheric radiative transfer, e.g. aerosol extinction, and surface reflectance.
4. Simulate  $\ln(I(\lambda)) - P_d(\lambda)$  with a radiative transfer model (RTM) and vary the atmospheric trace gas concentrations iteratively to fit the measurement within the instrument's measurement noise.

The last step represents the solution of the inverse problem of determining the atmospheric trace gas concentrations from the APEX measurements. Since there is not enough information in the measurement to determine the entire trace gas profiles, some regularisation has to be applied. Two obvious choices are to

- regularise the inversion explicitly with an a priori profile or some constraint on the smoothness or to
- assume an a priori profile shape and scale it during the inversion as in conventional DOAS.

In both cases, typical values of trace gas columns for the free troposphere plus the stratosphere may be retrieved for individual APEX scenes. We suggest to use these typical columns to subsequently regularise the retrieval of the trace gas abundance within the well-mixed planetary boundary layer (PBL) at high spatial resolution within the APEX scene. This approach is analog to the so-called reference sector method for the determination of the tropospheric column of NO<sub>2</sub> from, e.g., the GOME instrument aboard ESA's ERS-2 satellite [e.g. Richter and Burrows, 2002].

## Retrieval Precision Calculation

In order to analyse the precision of a method of the type outlined above we calculate the retrieval precision of a simultaneous least squares fit of the abundances of the relevant trace gases in the lowermost 1.5 km of the atmosphere.

The assumed fit windows are listed in Table 1 along with the spectral resolution  $\Delta\lambda$  and typical signal/noise ratios  $SNR$  at medium radiance levels. The instrument characteristics reflect the design status of summer 2004. The degree  $d$  of the polynomial used to remove the broadband characteristics is also listed. We also assume the observational scenario summarised in Table 2.

First, the sun-normalised radiance  $I_{bl}(\lambda)$  [1/sr] and its derivatives w.r.t. the trace gas concentration  $n_i$  [ $10^5/\text{cm}^3$ ] are calculated with the RTM SCARAYS [Kaiser and Burrows, 2003]. These

Table 1: Fit windows.

no.	wavelength range [nm]	$\Delta\lambda$ [nm]	$SNR$ [-]	degree $d$ of polynomial [-]
1	420–480	0.9	162	9
2	550–640	2.2	322	5
3	700–750	3.9	426	4
4	1550–1625	9.1	476	4
5	1625–1675	8.9	483	3
6	1980–2090	7.5	384	4
7	2090–2190	7.0	471	4
8	2280–2400	6.5	300	4
9	2400–2450	6.2	180	4

Table 2: Observation scenario.

atmospheric profiles	mid-latitude background
solar zenith angle	30 deg
viewing geometry	nadir
surface albedo	30 %
flight height	6 km
retrieval layer	0–1.5 km

calculations are performed with spectral resolutions between 0.2 and 0.001 nm in order to resolve the tropospheric absorption lines. The resulting spectra are plotted in the left column of Figure 2.

Second, the observed radiance  $I(\lambda)$  is calculated at APEX spectral points in the selected fitting windows by convolving  $I_{bl}(\lambda)$  with a boxcar function of width  $\Delta\lambda$ . Thus its derivatives w.r.t. the trace gas concentrations can also be obtained by convolution with the boxcar function. The resulting spectra are plotted in the left columns of Figures 3–11.

Taking the logarithm of radiance is skipped in the retrieval precision calculation since it would distort the measurement error statistics.

Then a polynomial is fitted to each of the radiance and derivative spectra in each fit window. The differential trace gas absorption signatures are extracted by subtracting the polynomials. They are shown in the right columns of Figures 3–11 for the individual fit windows.

The measurement vector  $\mathbf{y}$  and the weighting function matrix  $\mathbf{K}$  are obtained by appending the differential structures of the individual fit windows such that

$$\mathbf{y} - \mathbf{y}_a = \mathbf{K}(\mathbf{x} - \mathbf{x}_a) \quad , \quad (1)$$

where  $\mathbf{x}$  holds the six trace gas concentrations and  $\mathbf{x}_a$  and  $\mathbf{y}_a$  correspond to a suitable linearisation point, e.g. the a priori.  $\mathbf{y}$  and the columns of  $\mathbf{K}$  are plotted in the right column of Figure 2.

Now the a posteriori covariance matrix of a simultaneous least squares fit of the trace gas concentrations  $\mathbf{x}$  can be calculated as

$$\mathbf{S}_x = (\mathbf{K}^T \mathbf{S}_y^{-1} \mathbf{K})^{-1} \quad , \quad (2)$$

where  $\mathbf{S}_y$  denotes the measurement covariance matrix. It is calculated with the signal/noise ratio  $SNR$  from the simulated observed radiance  $I(\lambda)$  and assumed to be diagonal.

The theoretical retrieval precisions

$$\sigma_i = \sqrt{\mathbf{S}_x(i, i)} \quad (3)$$

are obtained from the diagonal elements of the a posteriori covariance matrix and the retrieval correlations

$$c_{i,j} = \sqrt{\frac{\mathbf{S}_x(i, j)}{\sigma_i \sigma_j}} \quad (4)$$

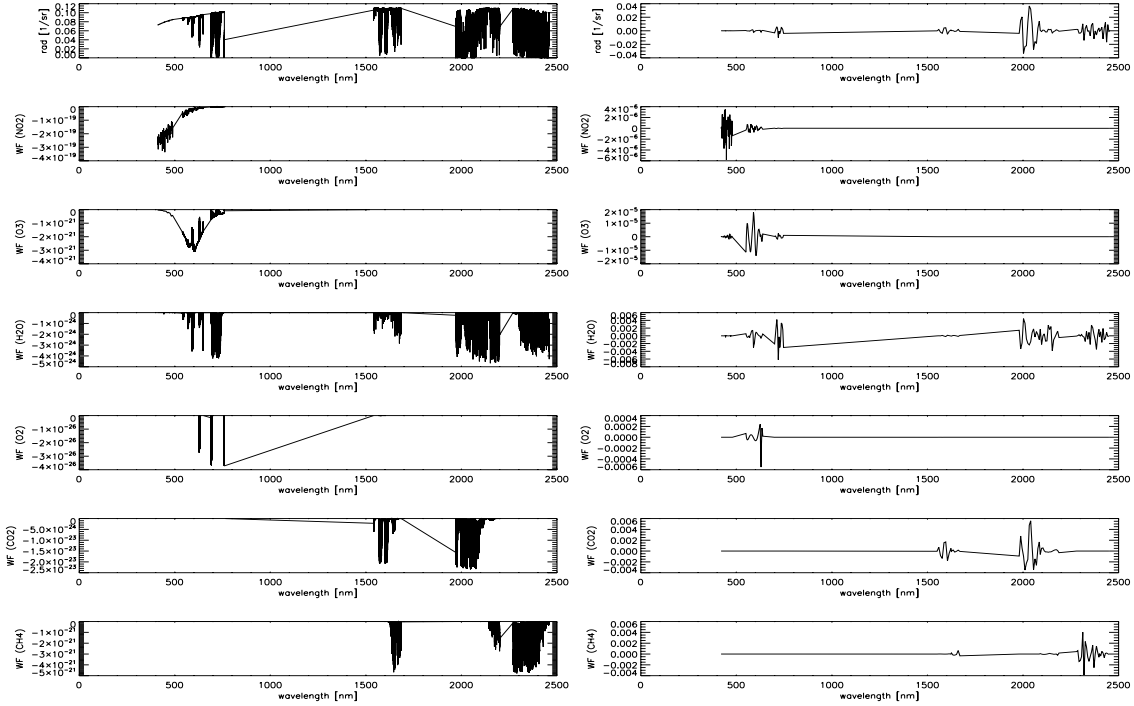


Figure 2: Left: Hi-resolution simulation of observed radiance and its derivatives w.r.t. the trace gases. Right: Differential structure of observed radiance at instrument resolution and its derivatives w.r.t. the trace gases.

from its off-diagonal elements.

## Results

The calculated theoretical retrieval precisions  $\sigma_i$  for the considered trace gases are listed in Table 3 in volume mixing ratio units and relative to the assumed background atmosphere. The correlations between the retrieved concentrations are shown in Table 4.

The atmospheric background of NO<sub>2</sub> cannot be detected with APEX. However, pollution events with abundances of up to 40 ppb have been reported by the ground stations of the Swiss NABEL network. [e.g. Schaub et al., 2005]. Such events will be observed and characterised accurately with APEX. The NO<sub>2</sub> retrieval errors show no significant correlation.

The retrieval precision of O<sub>3</sub> is of the same order of magnitude as the atmospheric background value. Therefore, quantitative observations of pollution events are anticipated. The retrieval error O<sub>3</sub> exhibits a clear correlation of 11 % with the one for H<sub>2</sub>O. This is a direct result of the correlated

Table 3: Theoretical Concentration Retrieval Precisions.

molecule	volume mixing ratio [ppm]	background [ppm]	pollution [ppm]
NO <sub>2</sub>	$7 \times 10^{-5}$	$2 \times 10^{-5}$	$4 \times 10^{-2}$
O <sub>3</sub>	0.015	0.026	
H <sub>2</sub> O	4	$5 \times 10^4$	
O <sub>2</sub>	7420	$2.1 \times 10^5$	
CO <sub>2</sub>	0.44	376	
CH <sub>4</sub>	0.01	1.8	

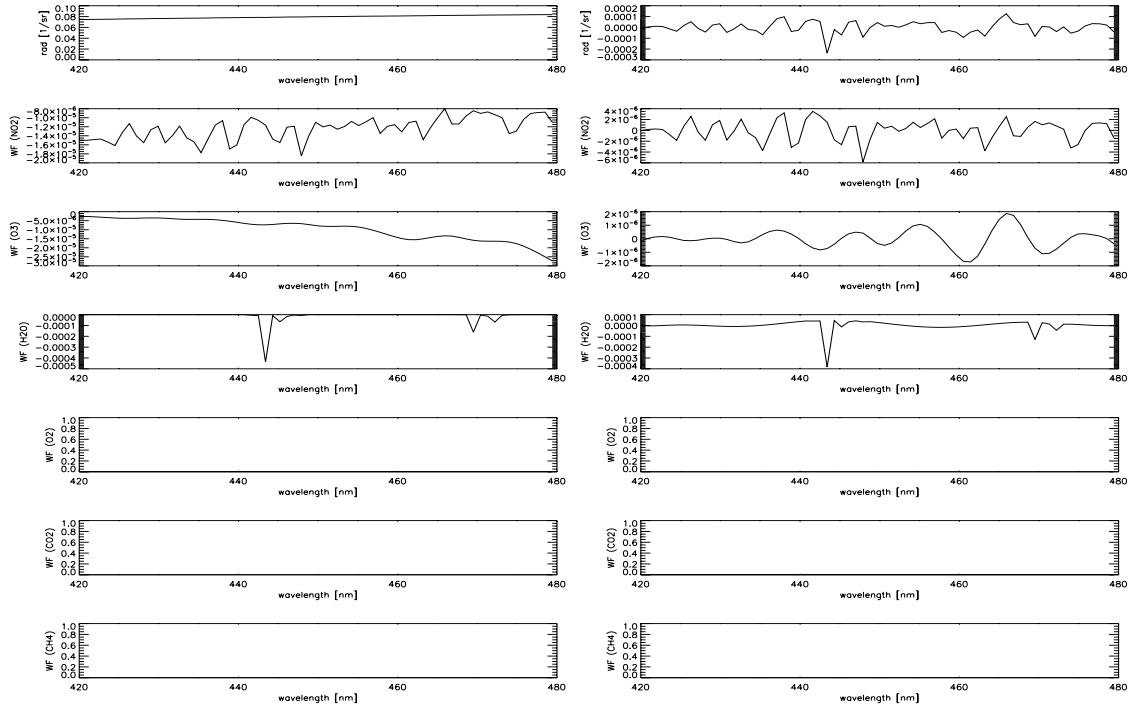


Figure 3: Radiance (top left) and its differential structure (top right) and the correspondig derivatives w.r.t. the trace gases NO<sub>2</sub>, O<sub>3</sub>, O<sub>2</sub>, H<sub>2</sub>O, CO<sub>2</sub>, and CH<sub>4</sub> for fit window 1.

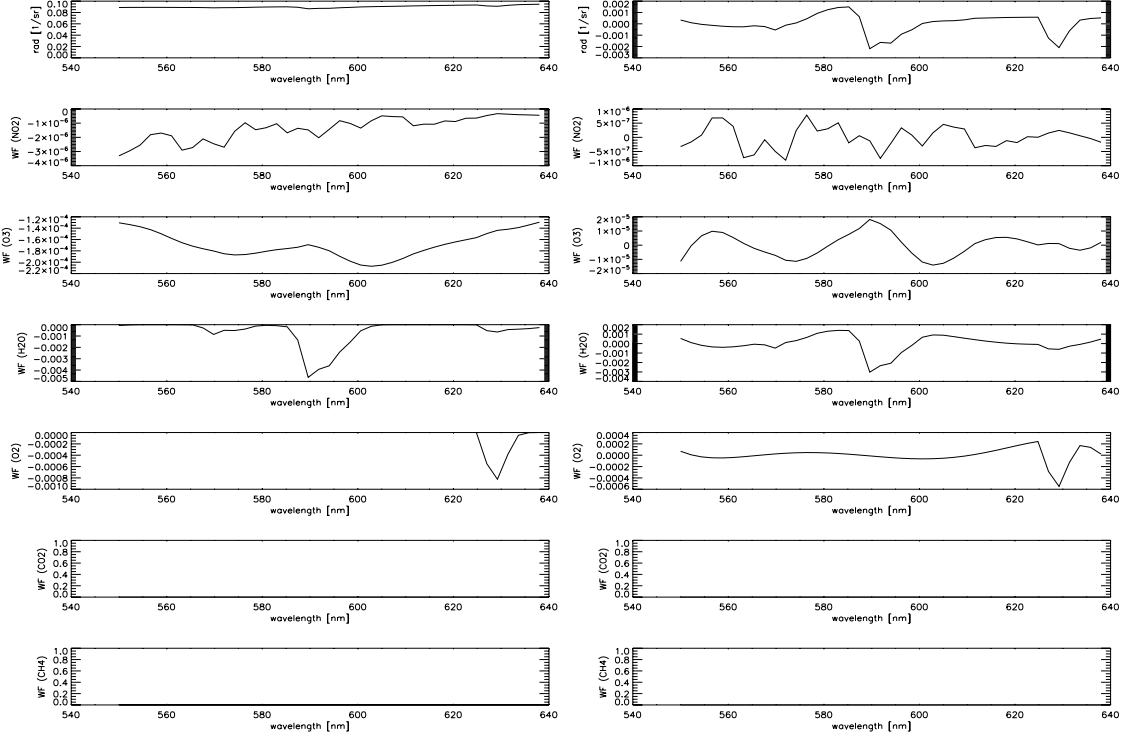


Figure 4: Same as Figure 3 for fit window 2.

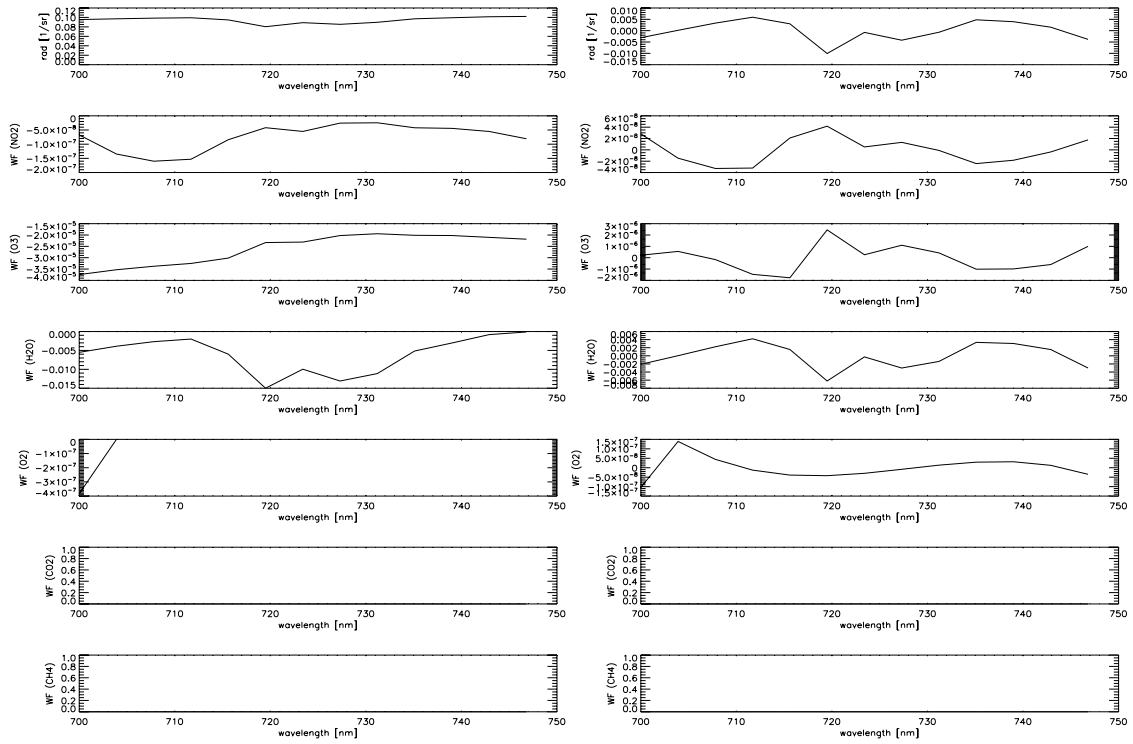


Figure 5: Same as Figure 3 for fit window 3.

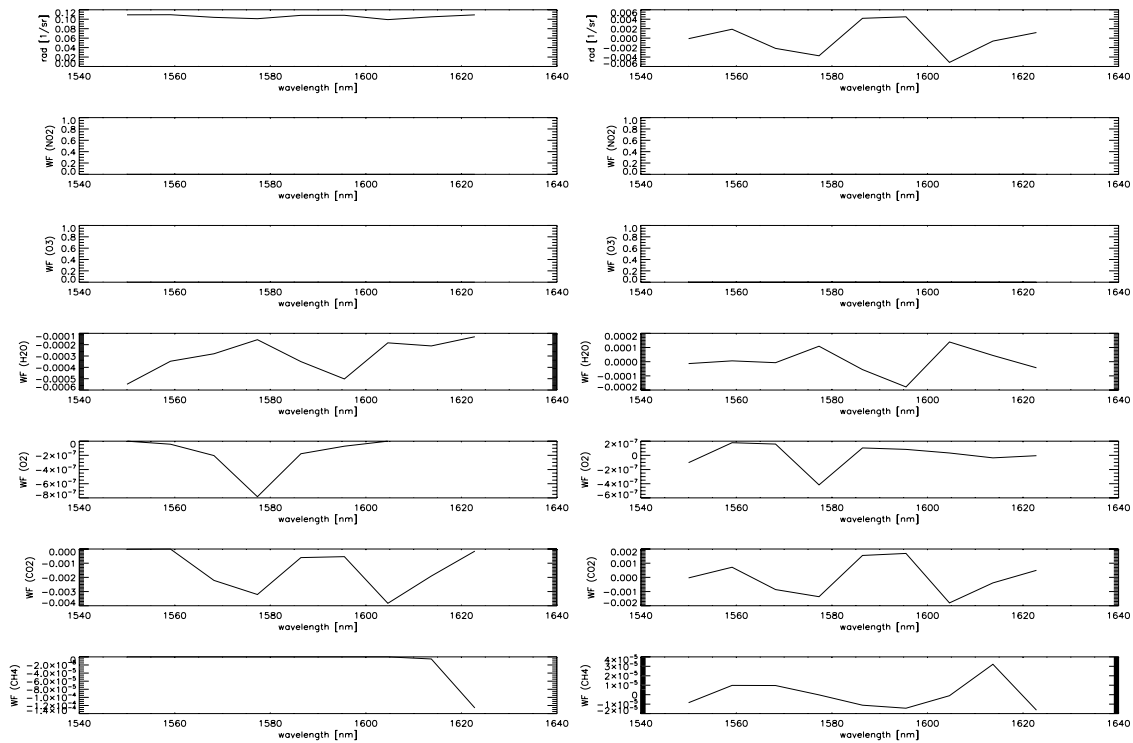


Figure 6: Same as Figure 3 for fit window 4.

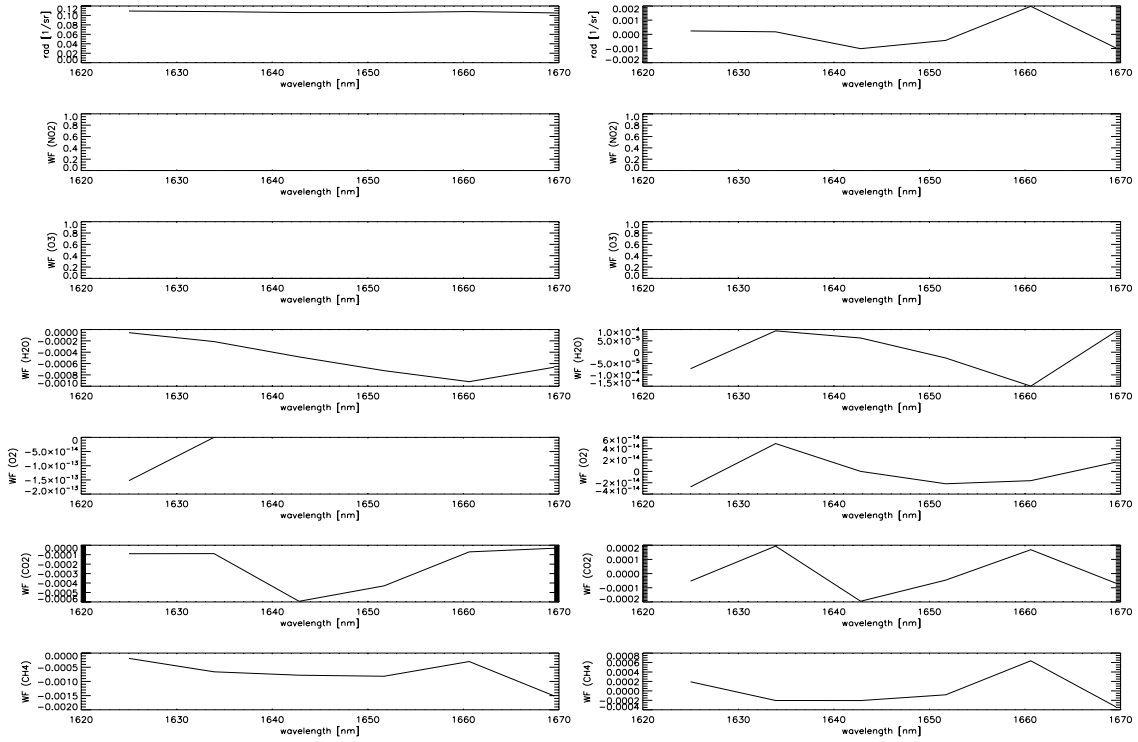


Figure 7: Same as Figure 3 for fit window 5.

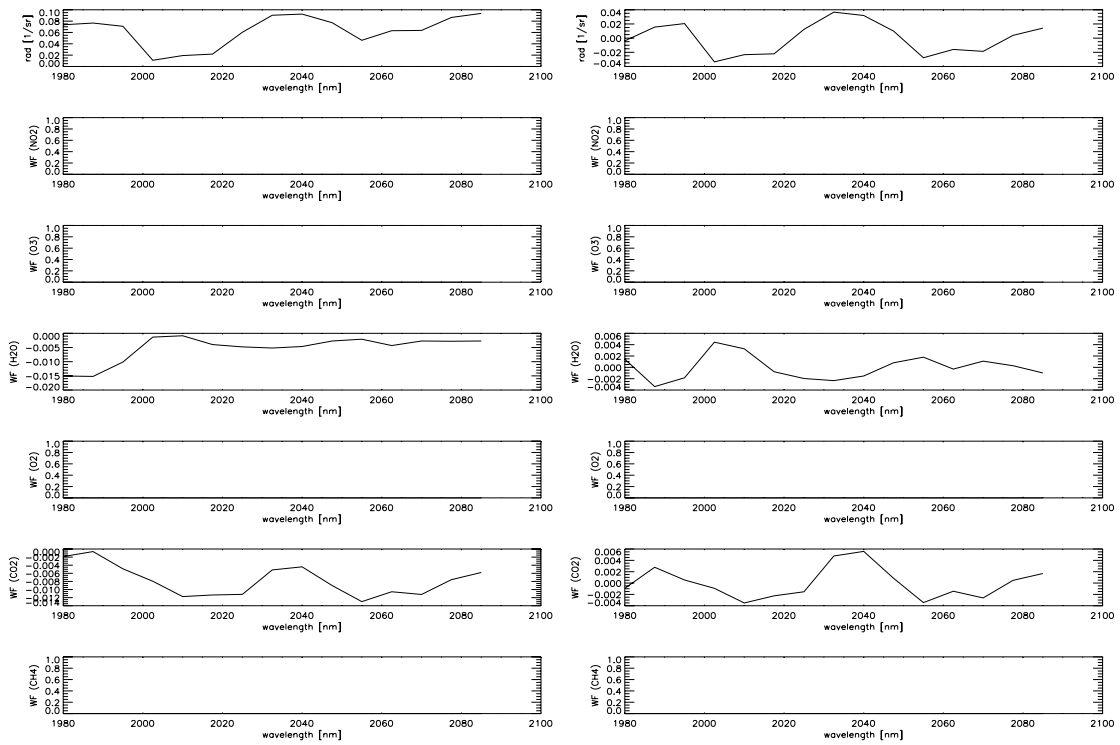


Figure 8: Same as Figure 3 for fit window 6.

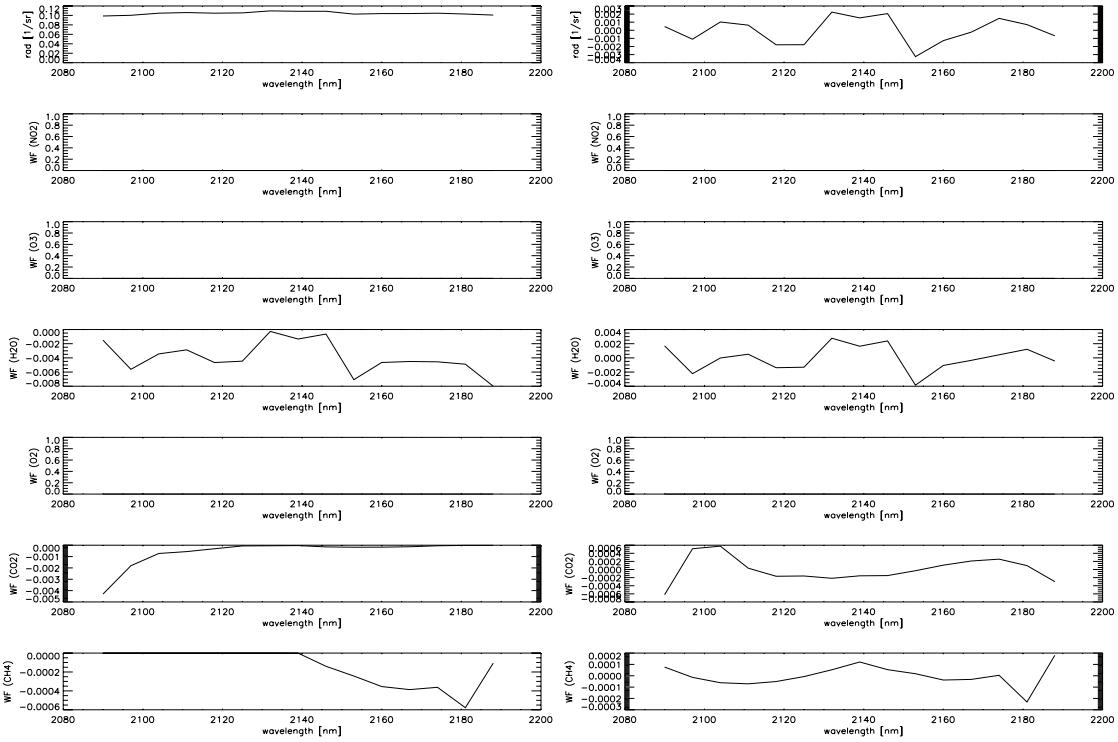


Figure 9: Same as Figure 3 for fit window 7.

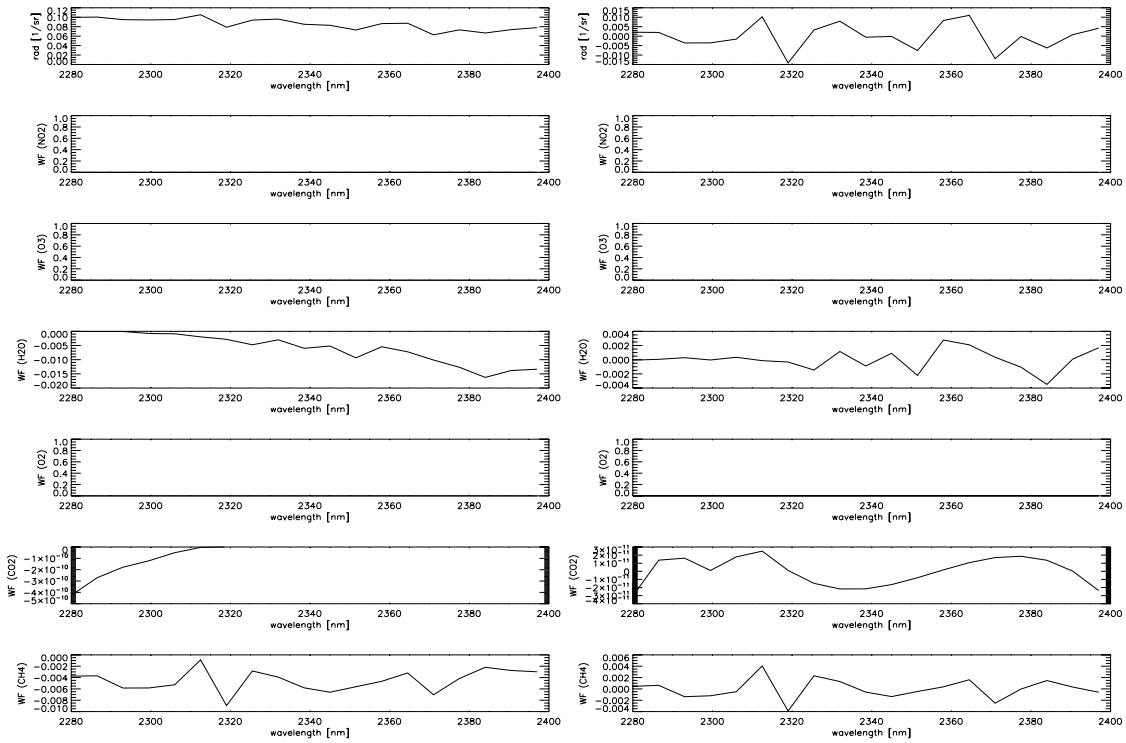


Figure 10: Same as Figure 3 for fit window 8.

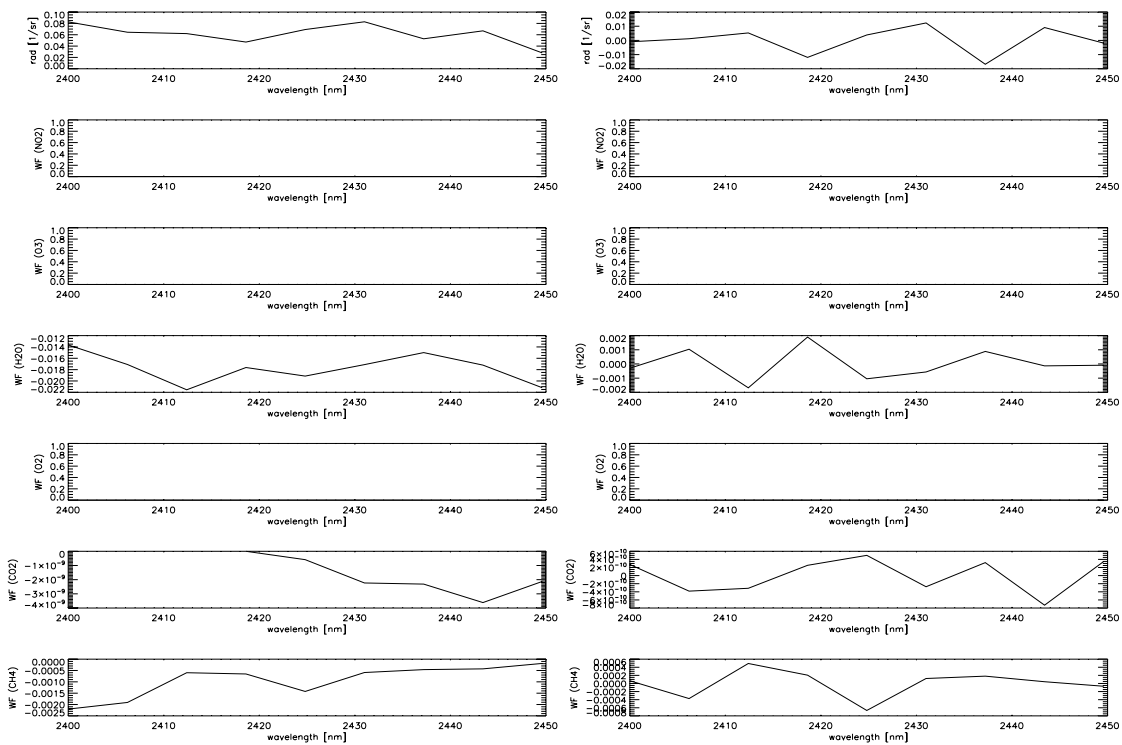


Figure 11: Same as Figure 3 for fit window 9.

Table 4: Theoretical Concentration Retrieval Error Correlations [%].

	NO2	O3	H2O	O2	CO2	CH4
NO2	100	2	-0.5	5	-0.3	-0.001
O3		100	11	2	6	0.2
H2O			100	-3	55	2
O2				100	-1	-0.05
CO2					100	1
CH4						100

absorption feature around 590 nm.

The retrieval of CO<sub>2</sub> concentrations appears to be more precise than 1%. This shows that it is not limited by the instrument's noise. Instead, systematic errors may dominate. Since they are subject to corrections it is anticipated that APEX will be capable of characterising important CO<sub>2</sub> sources and sinks. A relatively strong correlation with the H<sub>2</sub>O retrieval error stresses the importance of determining this the humidity correctly.

A similar argument holds for CH<sub>4</sub>, though it is free of significant correlations.

## Conclusions

The airborne imaging spectrometer APEX will record atmospheric radiance spectra in the wavelength range 380–2500 nm with a spectra resolution varying between 0.5 and 10 nm. The spectra are recorded simultaneously for 1000 across-track pixels with a pixel size of 2–5 m depending on flight altitude. The instrument will become operationally available in 2006.

The observations offer a unique opportunity to quantitatively observe the distributions of the atmospheric trace gases NO<sub>2</sub>, O<sub>3</sub>, CO<sub>2</sub>, and CH<sub>4</sub> in the planetary boundary layer (PBL). Thus sources and sinks of air pollution will be characterised with a resolution of down to a few meters while covering regions of several kilometers extend. Since the vertical structures within the PBL may not be resolved the observations may be smeared horizontally to a scale corresponding to the extent of vertical mixing. Nevertheless, APEX offers a new, greatly enhanced possibility to monitor local and regional air pollution.

Additionally, the distributions within entire satellite pixels may be characterized to validate the satellite instrument products and facilitate the down/up-scaling. Trace gas profile information may be obtained by observing the same scene with several flight altitudes.

The required retrieval algorithms can be based on the principles established for air pollution monitoring from satellite. They need, however, careful adaptation to the specific properties of APEX.

## Acknowledgments

The work in this paper is being carried out under ESA/ESTEC contract no. 15440/01/NL/Sfe. The support of the University of Zurich is acknowledged.

## References

- M. Buchwitz, V.V. Rozanov, and J.P. Burrows. A near-infrared optimized DOAS method for fast global retrieval of atmospheric ch<sub>4</sub>, co, co<sub>2</sub>, and n<sub>2</sub>o total column amounts from SCIAMACHY Envisat-1 nadir radiances. *J. Geophys. Res.*, 105(D12):15231–15245, 2000.
- J. Heldstab, P. de Haan, T. Künzle, N. Kljun, M. Keller, and R. Zbinden. *Modelling of NO<sub>2</sub> and benzene ambient concentrations in Switzerland 2000 to 2020*, volume 188 of *Environmental Documentation*. Swiss Agency for the Environment, Forests and Landscape SAEFL, CH-8003 Berne, 2004.
- R. Höller, A. Higurashi, and T. Nakajima. The GLI 380-nm channel application for satellite remote sensing of tropospheric aerosol. In *The 2004 EUMETSAT Meteorological Satellite Conference*, 2004.
- J.W. Kaiser and J.P. Burrows. Fast weighting functions for retrievals from limb scattering measurements. *J. Quant. Spectrosc. Radiat. Transfer*, 77(3):273–283, 2003.
- J.W. Kaiser, J. Nieke, D. Schlöpfer, J. Brazile, and K.I. Itten. The atmospheric sensitivity of the airborne imaging spectrometer APEX. In *Current Problems in Atmospheric Radiation*, Current Problems in Atmospheric Radiation. International Radiation Commission, 2004.

- Y.J. Kaufman, A.E. Wald, L.A. Remer, B.-C. Gao, R.-R. Li, and L. Flynn. The MODIS 2.1  $\mu\text{m}$  channel correlation with visible reflectance for use in remote sensing of aerosol. *IEEE Trans. Geosci. Remote Sensing*, 35(5):1286–1298, 1997.
- F. Lohberger, G. Hönninger, and U. Platt. Ground-based imaging differential optical absorption spectroscopy of atmospheric gases. *Appl. Opt.*, 43(24):4711–4717, 2004.
- R. Marion, R. Michel, and C. Faye. Measuring trace gas in plumes from hyperspectral remoteley sensed data. *IEEE Trans. Geosci. Remote Sensing*, 42(4), 2004.
- J. Nieke, K.I. Itten, J.W. Kaiser, D. Schläpfer, J. Brazile, W. Debruyne, K. Meuleman, P. Kempeneers, A. Neukom, H. Feusi, P. Adolph, R. Moser, T. Schillinger, M. van Quickenberghe, J. Alder, D. Moller, L. De Vos, P. Kohler, M. Meng, J. Piesbergen, P. Strobl, M.E. Schaepman, J. Gavira, and R. Meynar. APEX: Current status of the airborne dispersive pushbroom imaging spectrometer. *Proc. SPIE*, 5542, 2004.
- U. Platt. Differential optical absorption spectroscopy (DOAS). In M.W. Sigrist, editor, *Air Monitoring by Spectroscopic Techniques*, volume 127 of *Chem. Anal.*, pages 27–76. Wiley-Interscience, New York, 1994.
- A. Richter and J.P. Burrows. Tropospheric  $\text{NO}_2$  from some measurements. *Adv. Space Res.*, 29(11):1673–1683, 2002.
- D. Schaub, A.K. Weiss, J.W. Kaiser, A. Petritoli, A. Richter, B. Buchmann, and J.P. Burrows. A transboundary transport episode of nitrogen dioxide as observed from GOME and its impact in the Alpine region. *Atmos. Chem. Phys.*, 5:23–37, 2005.
- D. Schläpfer and M. Schaepman. Modeling the noise equivalent radiance requirements of imaging spectrometers based on scientific applications. *Appl. Opt.*, 41(27):5691–5701, 2002.
- C. E. Sioris, T. P. Kurosu, R. V. Martin, and K. Chance. Stratospheric and tropospheric  $\text{NO}_2$  observed by SCIAMACHY: First results. *Adv. Space Res.*, 34(4):780–785, 2004.
- W. von Hoyningen-Huene, M. Freitag, and J. P. Burrows. Retrieval of aerosol optical thickness over land surfaces from top-of-atmosphere radiance. *J. Geophys. Res. A*, 108(D9):4260, 2003.
- C. von Savigny, A.B. Davis, O. Funk, and K. Pfeilsticker. Time-series of zenith radiance and surface flux under cloudy skies: Radiative smoothing, optical thickness retrievals and large-scale stationarity. *Geophys. Res. Lett.*, 29(17):1825–1828, 2002.